Detectors

J. Synchrotron Rad. (1998). **5**, 845–847

Initial data from the 30-element ORTEC HPGe detector array and the XSPRESS pulse-processing electronics at the SRS, Daresbury Laboratory

R. C. Farrow,[a]* J. Headspith,[a] A. J. Dent,[a] B. R. Dobson,[a] R. L. Bilsborrow,[a] C. A. Ramsdale,[a] P. C. Stephenson,[a] S. Brierley,[a] G. E. Derbyshire,[b] P. Sangsingkeow[c] and K. Buxton[c]

[a]CLRC, Daresbury Laboratory, Warrington WA4 4AD, UK, [b]CLRC, Rutherford Appleton Laboratory, Chilton, Oxon OX11 0QX, UK, and [c]EG&G ORTEC, Midland Road, Oak Ridge, TN, USA. E-mail: r.c.farrow@dl.ac.uk

(*Received 4 August 1997; accepted 13 November 1997*)

Following the completion of the collaborative project between CLRC Daresbury Laboratory and EG&G ORTEC to develop the world's first 30-element HPGe detector for fluorescence XAFS, it has now been tested and commissioned at the SRS. The system was commissioned with the XSPRESS digital pulse-processing electronics and this has demonstrated processed count rates in excess of 10 MHz. Initial data have been recorded and are presented.

Keywords: detectors; adaptive digital signal processing; digital pulse-processing electronics; XAFS.

1. Introduction

XAFS is now a mature scientific technique, performed almost exclusively at synchrotron radiation sources, which gives information on the local structure around an atom of interest. Where the atom of interest is present in the sample in low concentrations, fluorescence XAFS is used. In the case of minimally scattering samples, such as dilute aqueous solutions, the lower XAFS analysis limit for the atom of interest is dictated by the intensity of X-rays delivered to the sample. However, if this intensity is sufficiently high or the sample scatters heavily, the limitation becomes the total throughput of the detection system.

Prior to the ultra-dilute spectroscopy (UDS) station 16.5 and the XSPRESS (Farrow *et al.*, 1995) detector system being available at the SRS, these lower limits were realistically around 1 m*M* for aqueous solutions and 1000 p.p.m. for highly scattering samples.

In order to reduce these limits we need to increase the photon processing rate of the system. However, if we are to do this without compromising the energy resolution of the system, few options are open. The 'brute force' approach is to increase the number of parallel detection channels (Cramer *et al.*, 1988; Derbyshire *et al.*, 1992). A more novel approach is to increase the efficiency of the signal processing chain by using optimized digital signal processing (Stein *et al.*, 1996). We have embraced both these approaches in the detector system for UDS at Daresbury and the increased processing rate that this yields, coupled with the increased flux available from the UDS station, allows us to push the concentration limits down significantly.

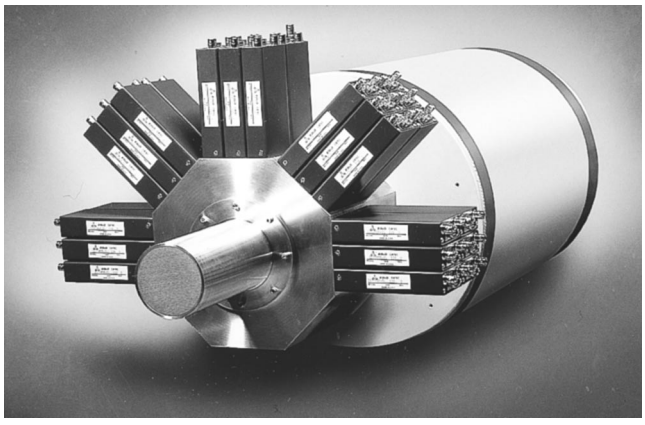

Figure 1
Photograph of the 30-element detector showing the entrance window and preamplifiers.

2. The 30-element XSPRESS detector system

2.1. *Detector*

The detector for ultra-dilute spectroscopy has been developed through a collaboration between EG&G ORTEC and CLRC Daresbury Laboratory. This detector has 30 parallel detection channels in a 50 mm diameter active area with each germanium crystal being 6 mm in diameter. A number of developments have been built into this detector in order to maximize its throughput,

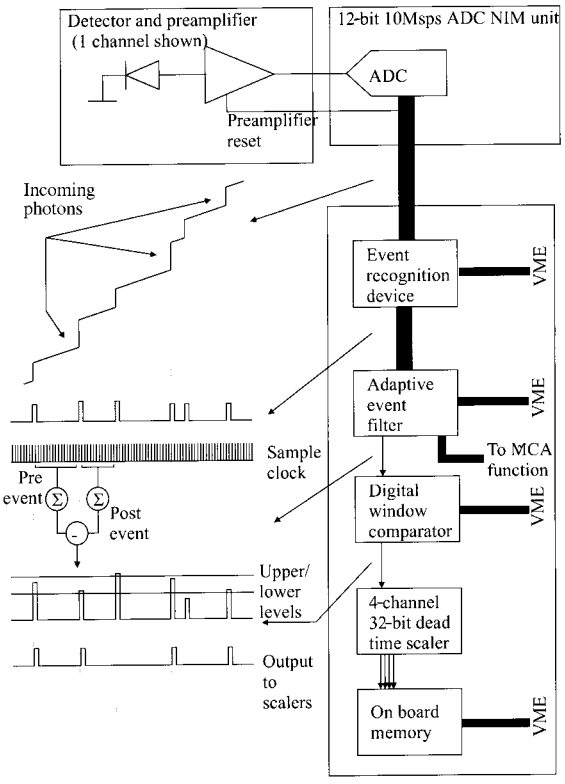

Figure 2
Block diagram showing operation of one channel of the XSPRESS digital pulse-processing system.

including high gain (12 mV keV^{-1}), low-rise-time (200 ns), fast-reset (3 μs) POF preamplifiers. The finished detector has an average energy resolution of 248 eV at Fe^{55} at 4 kHz input with a 0.5 μs shaping time constant. A photograph is given in Fig. 1.

2.2. *Signal processing*

The XSPRESS signal processing departs from the conventional fixed-dead-time analogue pulse processing by using adaptive digital signal processing techniques. These allow us to implement variable-bandwidth variable-dead-time algorithms for processing events.

The signal from the detector preamplifier is converted to a digital representation using a NIM-based 12-bit analogue-to-digital converter (ADC), sampling at 10 MHz. The resulting digital data are passed to the XSPRESS VME card where events are first recognized and then processed. The strength of the XSPRESS system is that for each event, the process algorithm used is selected according to the time available. Thus, for an event which is closely followed by a successive event, a very short, wide-bandwidth algorithm is used, whereas for an event that is essentially isolated, a much longer, narrow-bandwidth algorithm is used. This results in a system which suffers much less pileup than conventional systems allowing higher throughput, but where each event is processed to its optimum energy resolution. Fig. 2 shows a diagram of one channel of the system.

The throughput of this system is given by the following equation:

$$R_o = [R_i \exp(-T_d R_i)]\left[1 - \frac{R_i GE}{(DNR/T_r) - R_i GE}\right],$$

where R_o is the processed event output rate of the system, R_i is the incident photon rate on the detector, G is the event gain at the preamplifier output in mV keV^{-1}, E is the average energy of the input spectrum in keV, DNR is the dynamic range of the preamplifier, T_r is the reset time of the preamplifier with no incident photons, T_d is the minimum process dead time associated with each event.

The first half of the equation is the well known throughput equation of a paralysable detector system (Knoll, 1989). However, the second half is a correction required as the reset dead time in POF systems is not negligible at high rates and, as the system takes longer to reset at these rates, this becomes a significant effect.

Although T_d is a minimum process dead time, the processing may continue for a longer period. However, as the processing can take as little as T_d, it is this minimum value that dictates the maximum output rate.

The peak shapes obtained are different from those normally gained from fixed-dead-time algorithm systems. This is because the peaks within this system are due to the superposition of all the peaks arising from the different algorithms available to the system. As the input rate increases, the peak shape changes due to the use of different combinations of the algorithms. Fig. 3 gives a theoretical representation of the peak shape at four different input rates.

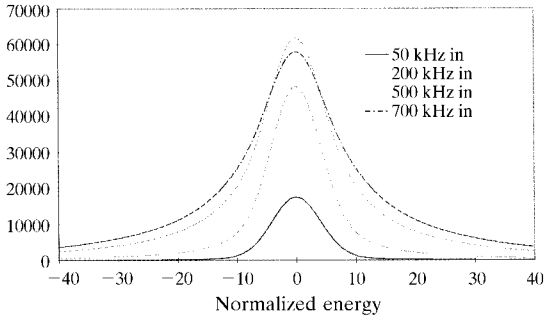

Figure 3
Diagram showing how the output peak shape changes with rate for the XSPRESS system.

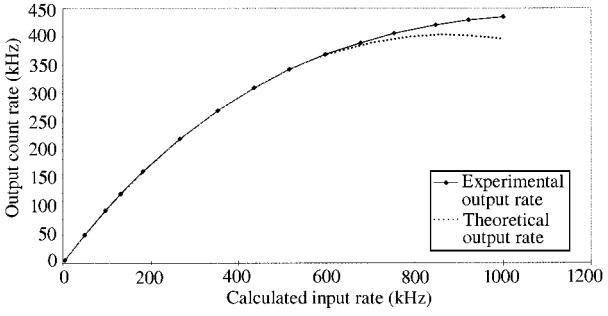

Figure 4
Graph showing the average throughput of all 30 channels of the XSPRESS system at Zr $K\alpha$ (15.77 keV).

3. Tests

3.1. *System performance*

In order to evaluate the operating parameters of the system, the detector collected fluorescence and scattered radiation from a zirconium foil. The intensity of the radiation was varied by opening or closing the slits which defined the size of the incident beam. The input rate was calculated from the ion-chamber output and the dead-time-corrected intensity was recorded for a range of input intensities. Figs. 4, 5 and 6 indicate how the output rate, the energy resolution and the peak shift all vary with input rate. In

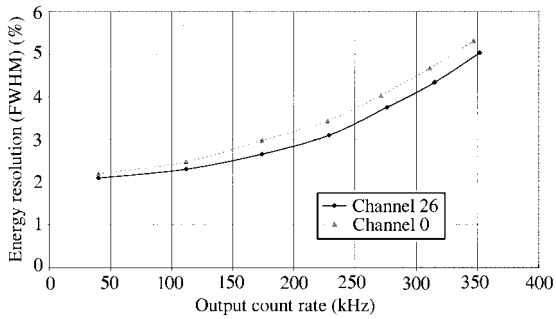

Figure 5
Graph showing the FWHM resolution against output rate of two randomly selected channels of the XSPRESS system at Zr $K\alpha$ (15.77 keV).

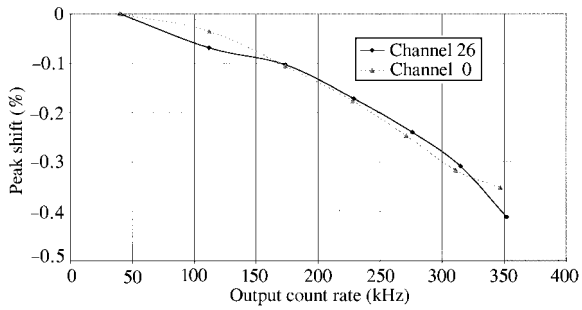

Figure 6
Graph showing the peak shift against output rate of two randomly selected channels of the XSPRESS system at Zr $K\alpha$ (15.77 keV).

Fig. 4, an average of all 30 channels was used; however, in Figs. 5 and 6, randomly selected channels 0 and 26 were used.

3.2. *Dilute aqueous solution*

In order to demonstrate the use of the system for XAFS, a number of scans of aqueous $K_2(Pt)Cl_4$ were collected. Fig. 7 shows the background-subtracted XAFS of a 100 m*M* solution which has been collected at output rates of 10, 44 and 192 kHz. In each case the data comprise a single scan collected in 20 min.

4. Results and discussion

Fig. 4 shows that the system throughput fitted well to the theory if a process dead time of 450 ns and a reset dead time of 3.12 μs were assumed. Deviation at the top of the graph was probably due to multiple events occurring within the resolving time of the processor.

The resolution in Fig. 5 was slightly worse than calculated (~2.1% as opposed to 1.8%) but this was probably due to the ADCs running under sub-optimal conditions. The peak shift in Fig. 6 was within the calculated limits for the system.

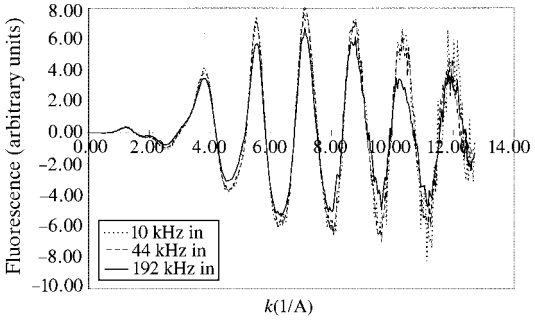

Figure 7
Comparison of background-subtracted XAFS of 100 m*M* $K_2(Pt)Cl_4$ solution taken at three different input rates.

Although the comparison of the XAFS of the Pt solution in Fig. 7 showed close correlation of the collected data, the process dead time used in the relinearization algorithm was too short (300 ns) and as such the amplitudes of the oscillations were still compressed slightly at higher rates.

The system is presently undergoing further final commissioning and these results are very much preliminary. Optimum performance will be achieved by improving a number of parameters, including energy resolution, where cooling issues with the ADC units are being addressed, fluorescence windowing, where channel gains need fine trimming, and relinearization, where an ideal processing value for each channel will be determined and used.

5. Conclusions

We have presented data from the world's first 30-element high-purity detector for fluorescence XAFS combined with the XSPRESS digital signal processing electronics. This has only come about through both an extensive collaboration between EG&G ORTEC and CLRC and the development of highly efficient digital pulse-processing techniques.

References

Cramer, S. P., Tench, O., Yocum, M. & George, G. N. (1988). *Nucl. Instrum. Methods*, A**266**, 586–591.

Derbyshire, G. E., Dent, A. J., Dobson, B. R., Farrow, R. C., Felton, A., Greaves, G. N., Morrell, C. & Wells, M. P. (1992). *Rev. Sci. Instrum.* **63**, 814–815.

Farrow, R., Derbyshire, G. E., Dobson, B. R., Dent, A. J., Bogg, D., Headspith, J., Lawton, R., Martini, M. & Buxton, K. (1995). *Nucl. Instrum Methods*, B**97**, 567–571.

Knoll, G. F. (1989). *Radiation Detection and Measurement*. New York: Wiley.

Stein, J., Scheuer, F., Gast, W. & Georgiev, A. (1996). *Nucl. Instrum. Methods*, B**113**, 141–145.